Reflectivity properties of an abruptly ended asymmetrical slab waveguide for the case of transverse magnetic modes

G. Latsas

University of Athens, Department of Physics, Applied Physics Division, Electronics Laboratory, Building V, Panepistimiopolis, 157 84 Zografou, Athens, Greece

A. B. Manenkov

Institute for Physical Problems, Russian Academy of Sciences, Ulitsa Kosygina 2, Moscow, 117973 GSP-1, Russia

I. G. Tigelis and E. Sarri

University of Athens, Department of Physics, Applied Physics Division, Electronics Laboratory, Building V, Panepistimiopolis, 157 84 Zografou, Athens, Greece

Received April 13, 1999; accepted July 2, 1999; revised manuscript received August 23, 1999

We deal with the scattering phenomenon from an abruptly terminated asymmetrical slab waveguide for the case of transverse magnetic (TM) modes. The analysis uses both the integral equation method and the variational technique. The reflection coefficient of the dominant TM guided mode and the far-field radiation pattern are computed, and the discontinuity of the electric field distribution on the core–clad interface is exhibited. Numerical results are presented for several cases of abruptly ended waveguides, including the three-layer slab guide and the structure with variable profile of the refractive index. © 2000 Optical Society of America [S0740-3232(00)00801-2]

OCIS codes: 060.2310, 130.2790, 130.3120, 230.4170, 230.7370, 230.7390, 230.7400, 350.5500, 350.5610.

1. INTRODUCTION

Many different methods have been developed to deal with the discontinuity problems encountered in integrated optics.[1–7] By the term discontinuity problems, we mean the abrupt changes in the cross section, the refractive-index changes in the waveguide core or cladding, the bending of a waveguide, etc. In the past the problem of the scattering of transverse electric (TE) or transverse magnetic (TM) modes by a semi-infinite symmetrical slab waveguide was solved by several authors,[8–12] while similar problems for cylindrical geometry were also investigated.[13–15] Furthermore, extensive research has been made for the coupling phenomena between symmetrical or asymmetrical waveguides, where either both are planar,[16] both are circular,[17,18] or one is circular and one is planar.[19] Finally, the scattering phenomenon from an abruptly terminated three-layer slab waveguide for the case of TE modes has recently been solved by both the integral equation method and the variational technique.[20]

In the present work the reflectivity properties of an abruptly ended asymmetrical slab waveguide for the case of the dominant TM guided mode are analyzed by both the integral equation method and the variational technique. It has to be mentioned that this problem has significant practical interest, since such systems find wide application in integrated optics. Note also that there exist new, potentially interesting effects (such as asymmetry of the far-field pattern, etc.) for asymmetrical geometry, which are lacking in symmetrical problems. Finally, in the case of TM modes the electric field distribution has a discontinuity in the edge points on the terminal plane.

In Section 2 the radiation characteristics of an abruptly terminated asymmetrical slab waveguide (Fig. 1) are treated in detail by the integral equation method. In particular, an incident TM guided mode is assumed to propagate inside the slab waveguide toward the terminal plane $z = 0$. The existence of the axial discontinuity excites radiation waves and a guided mode propagating along the negative z axis. As a consequence, a mixed spectrum of eigenwaves is employed to describe the induced electromagnetic field inside the waveguide.[21] On the other hand, the fields in the semi-infinite region ($z > 0$) are expressed in terms of free-space eigenwaves (i.e., plane waves). Then a well-known procedure[20] is followed, and a Fredholm integral equation of the second kind is obtained for the unknown transverse electric field distribution $E_x(x, z = 0)$ on the terminal plane of the waveguide in a form suitable for developing a Neumann-series solution. This procedure is applied up to third order and yields very accurate results, especially when the weak guiding condition is satisfied. Then the reflection coefficient of the guided mode, the far-field radiation pattern, and the transverse electric field distribution on the terminal plane are computed.

0740-3232/2000/010162-11$15.00

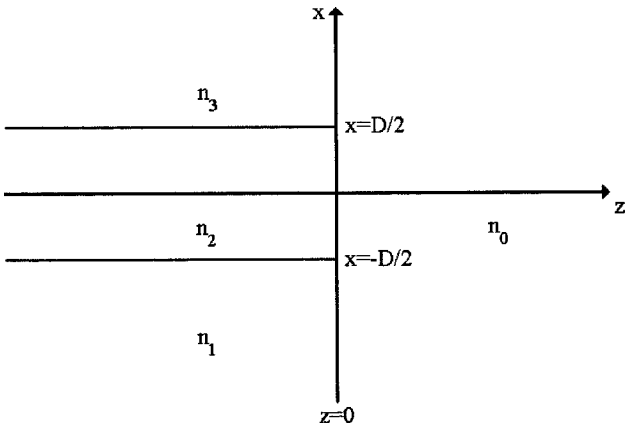

Fig. 1. Geometry of an abruptly ended asymmetrical slab waveguide.

In Section 3 the problem in question is treated by the variational technique,[8,13,14,22] which is based on the same equations (the eigenwave expansions and the integral equation for the electric field on the terminal plane) as those with the integral equation method. This technique is an approximate method and does not give a complete solution of the problem, for example for the outward radiation pattern. However, it has some advantages: It is simple and can be applied to problems with complicated geometry (for example, abruptly ended fibers, anisotropic waveguides,[13,15,22] etc.). In addition, this technique has already been employed to study the abruptly terminated asymmetrical planar guide with constant and variable profiles of the refractive index.[20] Note that the last profile of dielectrics frequently occurs because of the diffusive process during manufacture of the waveguides.

2. INTEGRAL EQUATION METHOD

The geometry of the problem under consideration is presented in Fig. 1. In particular, a three-layer slab waveguide ($z < 0$) is abruptly terminated at the plane $z = 0$ and radiates into the homogeneous semi-infinite region $z > 0$. The core region of the waveguide is assumed to have a refractive index n_2 and width D and is deposited on an infinitely wide substrate with a refractive index n_1. The refractive index of the medium above the core ($x > D/2$) is indicated as n_3. To achieve true mode guidance, n_2 should be larger than n_1 and n_3. In the present paper we have chosen $n_2 > n_1 \geqslant n_3$. If $n_1 = n_3$, obviously the waveguide is reduced to that of a symmetrical slab. On the other hand, the semi-infinite region $z > 0$ is considered to be homogeneous and have a refractive index equal to n_0. The whole space is assumed to be magnetically homogeneous with a magnetic permeability $\mu_0 = 4\pi \times 10^{-7}$ H/m. In the following analysis a harmonic time dependence $\exp(+j\omega t)$ is supposed and suppressed for the electromagnetic field quantities, while the free-space wave number is denoted by $k_0 = \omega/c$, where c is the velocity of light in vacuum.

Since the slab is assumed to be infinitely extended in the y direction, all field quantities are independent of y ($\partial/\partial y \equiv 0$) and the electromagnetic field can be decomposed in terms of TE and TM modes. In an asymmetrical slab waveguide, these modes are more complicated than those of a symmetrical one, since in the latter they can be expressed as either even or odd field distributions.[21] Furthermore, the lowest-order mode of an asymmetrical slab waveguide has a nonzero cutoff frequency, which means that this mode cannot propagate at arbitrarily low frequencies. In the present paper, only one TM guided mode is taken into account. For this case, only a single component of the magnetic field, parallel to the y axis, exists and is given by

$$H_{yg}(x, z) = \frac{\omega\epsilon_0}{\beta_0} U_0(x)\exp(-j\beta_0 z), \tag{1}$$

where ϵ_0 is the dielectric constant of the free space,

$$U_0(x) = A\begin{cases} \exp[-h_3(x - D/2)], & x \geqslant D/2 \\ \cos[h_2(x - D/2)] - (h_3/h_2)(n_2/n_3)^2 \sin[h_2(x - D/2)], & |x| \leqslant D/2, \\ [\cos(h_2 D) + (h_3/h_2)(n_2/n_3)^2 \sin(h_2 D)]\exp[h_1(x + D/2)], & x \leqslant -D/2 \end{cases} \tag{2}$$

and $h_1^2 = \beta_0^2 - k_0^2 n_1^2$, $h_2^2 = k_0^2 n_2^2 - \beta_0^2$, and $h_3^2 = \beta_0^2 - k_0^2 n_3^2$, where β_0 is the axial wave number, which satisfy the equation

$$\left(\frac{h_2^2}{n_2^4} - \frac{h_1 h_3}{n_1^2 n_3^2}\right)\tan(h_2 D) = \frac{h_2}{n_2^2}\left(\frac{h_1}{n_1^2} + \frac{h_3}{n_3^2}\right) \tag{3a}$$

or the equivalent,

$$h_2 D = \cos^{-1}\left(\frac{h_2/n_2^2}{V_{21}}\right) + \cos^{-1}\left(\frac{h_2/n_2^2}{V_{23}}\right), \tag{3b}$$

with

$$V_{21} = \left(\frac{h_2^2}{n_2^4} + \frac{h_1^2}{n_1^4}\right)^{1/2}, \qquad V_{23} = \left(\frac{h_2^2}{n_2^4} + \frac{h_3^2}{n_3^4}\right)^{1/2}. \tag{4}$$

Note that Eqs. (1)–(3) have been derived by taking into account the boundary conditions at the interfaces $x = \pm D/2$. The expansion coefficient A can be obtained from the normalization condition

$$\int_{-\infty}^{+\infty} \frac{U_0^2(x)}{n^2(x)}\,dx = 1, \tag{5}$$

where

$$n(x) = \begin{cases} n_3, & x > D/2 \\ n_2, & |x| < D/2. \\ n_1, & x < -D/2 \end{cases} \tag{6}$$

It should be mentioned that in this problem the electric field has two components, one parallel to the propagation z axis (E_z) and one parallel to the x axis (E_x).

As mentioned in Section 1, the existence of the axial discontinuity at the plane $z = 0$ inevitably excites radiation waves and a guided mode propagating along the negative z axis opposite the incident wave direction. Therefore the radiation waves should also be included in the description of the field inside the waveguide region. These waves are, in general, described by a continuous spectrum of eigenwaves. Considering the nondepolarizing nature of the abrupt termination and the z-directed propagation of the incident wave, only one component, also parallel to the y axis, of the magnetic field is needed to describe the radiation waves in the waveguide region. The expressions of these waves can be easily found in the literature,[21] and therefore they are omitted in this paper. Nevertheless, we quote the orthogonality relations satisfied by the mixed spectrum of eigenwaves:

$$\int_{-\infty}^{+\infty} \frac{\Psi_m(x,\rho)\Psi_k(x,\rho')}{n^2(x)}\,\mathrm{d}x = \delta_{mk}\delta(\rho-\rho'), \qquad m,k = 1,2, \quad (7a)$$

$$\int_{-\infty}^{+\infty} \frac{U_0(x)\Psi_m(x,\rho)}{n^2(x)}\,\mathrm{d}x = 0, \qquad m = 1,2, \quad (7b)$$

$$U_0(x)U_0(x') + \sum_{m=1}^{2}\int_{\rho_m}^{+\infty}\Psi_m(x,\rho)\Psi_m(x',\rho)\,\mathrm{d}\rho = n^2(x)\delta(x-x'), \quad (7c)$$

where $\rho_1 = 0$, $\rho_2 = k_0\sqrt{{n_1}^2 - {n_3}^2}$, $\Psi_m(x,\rho)(m = 1,2, \rho_m < \rho < +\infty)$ is the eigenfunction of the radiation waves, ρ is the transverse wave number of the radiation waves, δ_{mk} is the Kronecker symbol, and $\delta(\rho-\rho')$ is the Dirac delta function. Note that if $\rho < \rho_2$, there is only one branch of the radiation waves of the waveguide, whereas if $\rho > \rho_2$, two terms must be included in the radiation field expansion.[21]

According to the above discussion, the total magnetic field in the waveguide region is written as

$$H_y^{\mathrm{I}}(x,z) = \frac{\omega\epsilon_0}{\beta_0}U_0(x)[\exp(-j\beta_0 z) - R_0\exp(+j\beta_0 z)] - \sum_{m=1}^{2}\int_{\rho_m}^{+\infty}\frac{\omega\epsilon_0}{\beta(\rho)}R_m(\rho)\Psi_m(x,\rho) \times \exp[+j\beta(\rho)z]\,\mathrm{d}\rho, \quad (8)$$

where

$$\beta^2(\rho) = {k_0}^2{n_1}^2 - \rho^2 \qquad (\rho_m < \rho < +\infty). \quad (9)$$

The first term on the right-hand side of Eq. (8) represents the incident wave, while the second and third terms are the reflected guided mode and the reflected radiation modes, respectively. The summation in Eq. (8) is used in order that all the radiation modes are included. Note that $\mathrm{Re}[\beta(\rho)] > 0$ and $\mathrm{Im}[\beta(\rho)] < 0$ in order that the radiation conditions are satisfied and to have outgoing waves. Finally, R_0 and $R_m(\rho)$ are unknown expansion coefficients to be determined.

In the semi-infinite region $z > 0$, only one component of the magnetic field, also parallel to the y axis, is taken into account, and it can be written as a Fourier integral:

$$H_y^{\mathrm{II}}(x,z) = \sum_{l=1}^{2}\int_0^{+\infty}\frac{\omega\epsilon_0}{\gamma(s)}T_l(s)\varphi_l(x,s)\exp[-j\gamma(s)z]\,\mathrm{d}s, \quad (10)$$

where $\gamma^2(s) = {k_0}^2{n_0}^2 - s^2$ $(0 < s < +\infty)$, $\mathrm{Re}[\gamma(s)] > 0$, $\mathrm{Im}[\gamma(s)] < 0$, $T_1(s)$, $T_2(s)$ are unknown expansion coefficients to be determined, and $\varphi_1(x,s) = (n_0/\sqrt{\pi})\cos(sx)$, $\varphi_2(x,s) = (n_0/\sqrt{\pi})\sin(sx)$ are the free-space eigenwaves satisfying the orthogonality relations:

$$\int_{-\infty}^{+\infty}\frac{\varphi_m(x,s)\varphi_k(x,s')}{{n_0}^2}\,\mathrm{d}x = \delta_{mk}\delta(s-s'), \qquad m,k = 1,2, \quad (11)$$

$$\int_0^{+\infty}\frac{\varphi_1(x,s)\varphi_1(x',s) + \varphi_2(x,s)\varphi_2(x',s)}{{n_0}^2}\,\mathrm{d}s = \delta(x-x'). \quad (12)$$

The corresponding expressions of the transverse electric field distribution $E_x(x,z)$ in the waveguide and semi-infinite regions are given by

$$E_x^{\mathrm{I}}(x,z) = \frac{1}{n^2(x)}U_0(x)[\exp(-j\beta_0 z) + R_0\exp(+j\beta_0 z)] + \frac{1}{n^2(x)}\sum_{m=1}^{2}\int_{\rho_m}^{+\infty}R_m(\rho)\Psi_m(x,\rho) \times \exp[+j\beta(\rho)z]\,\mathrm{d}\rho, \quad (13)$$

$$E_x^{\mathrm{II}}(x,z) = \frac{1}{{n_0}^2}\sum_{l=1}^{2}\int_0^{+\infty}T_l(s)\varphi_l(x,s)\exp[-j\gamma(s)z]\,\mathrm{d}s. \quad (14)$$

Following a well-known procedure[20] and using the orthogonal properties of $\{U_0(x),\Psi_m(x,\rho),\varphi_1(x,s),\varphi_2(x,s)\}$, we derive the following Fredholm integral equation of the second kind for the transverse electric field distribution $E_x(x,z=0) = \mathcal{E}(x)$ on the plane $z = 0$:

$$\mathcal{E}(x) = \mathcal{E}_0(x) + \int_{-\infty}^{+\infty}\mathcal{E}(x')K(x,x')\,\mathrm{d}x', \quad (15)$$

where

$$\mathcal{E}_0(x) = \frac{2Y_1}{\mathrm{par}(x)}U_0(x), \tag{16}$$

$$K(x,x') = -\frac{1}{\mathrm{par}(x)}\left\{(Y_1 - Y_{10})U_0(x)U_0(x') + \sum_{m=1}^{2}\int_{\rho_m}^{+\infty}[Y(\rho) - Y_{10}]\Psi_m(x,\rho)\Psi_m(x',\rho)\,\mathrm{d}\rho + \sum_{l=1}^{2}\int_{0}^{+\infty}[Y_0(s) - Y_{00}]\varphi_l(x,s)\varphi_l(x',s)\,\mathrm{d}s\right\}, \tag{17}$$

with

$$Y_1 = \frac{\omega\epsilon_0}{\beta_0}, \qquad Y(\rho) = \frac{\omega\epsilon_0}{\beta(\rho)},$$

$$Y_0(s) = \frac{\omega\epsilon_0}{\gamma(s)}, \qquad Y_{10} = \frac{\omega\epsilon_0}{k_0 n_1}, \qquad Y_{00} = \frac{\omega\epsilon_0}{k_0 n_0}, \tag{18}$$

$$\mathrm{par}(x) = Y_{10}n^2(x) + Y_{00}{n_0}^2. \tag{19}$$

In the limiting case where $n_2 = n_1 = n_3$, the physical problem treated in this paper is reduced to the simple case of reflection from a dielectric half-space. In this case the incident wave becomes a plane wave $\exp(-jk_0n_1z)$, and the electric field on the plane $z = 0$ is given from the first term on the right-hand side of Eq. (15). Therefore it is reasonable to expect that, when $n_3 \approx n_1 \approx n_2$, the exact solution $\mathcal{E}(x)$ would not differ significantly from $\mathcal{E}_0(x)$. Consequently, in integrated optics applications, where $n_1 \approx n_2 \approx n_3$, a method of successive-order approximations could be used to solve Eq. (15); i.e., the electric field could be written in the form

$$\mathcal{E}_N(x) = \mathcal{E}_0(x) + \sum_{i=1}^{N} C_i(x), \qquad N = 1,2,3, \tag{20}$$

with

$$C_i(x) = \int_{-\infty}^{+\infty}\mathrm{d}x_1\int_{-\infty}^{+\infty}\mathrm{d}x_2\cdots\int_{-\infty}^{+\infty}\mathrm{d}x_i\,K(x,x_1)K(x_1,x_2)\cdots K(x_{i-1},x_i)\mathcal{E}_0(x_i). \tag{21}$$

We can validate the solution described above on the basis of the following considerations. Under the condition where $n_3 \approx n_1 \approx n_2$, the characteristic transverse size Δ of the guided-mode field distribution is large: $k_0\Delta \gg 1$, where $\Delta \sim \min(1/h_j)$, $j = 1,2,3$. In this case the spectra of the radiation modes are narrow, i.e., $\rho < 1/\Delta \ll k_0n_2$ and $s < 1/\Delta \ll k_0n_0$; therefore $\beta(\rho) \approx k_0n_1$, $\gamma(s) \approx k_0n_0$ [see Eq. (9)], and $Y(\rho) \approx Y_{10}$, $Y_0(s) \approx Y_{00}$ [see Eqs. (18)]. Hence the integral equation kernel $K(x,x')$ is small, and we can use the iteration procedure described above. In this paper iterations up to third order have been computed, but only the expression of the first-order solution of the transverse electric field distribution is given below:

$$\mathcal{E}_1(x) = \mathcal{E}_0(x) - \frac{2Y_1}{\mathrm{par}(x)}\left\{(Y_1 - Y_{10})U_0(x)\left(\frac{UU}{\mathrm{par}}\right) + \sum_{m=1}^{2}\int_{\rho_m}^{+\infty}[Y(\rho) - Y_{10}]\Psi_m(x,\rho)\left(\frac{U\Psi_m}{\mathrm{par}}\right)\mathrm{d}\rho + \sum_{l=1}^{2}\int_{0}^{+\infty}[Y_0(s) - Y_{00}]\varphi_l(x,s)\left(\frac{U\varphi_l}{\mathrm{par}}\right)\mathrm{d}s\right\}, \tag{22}$$

where

$$\frac{UU}{\mathrm{par}} = \int_{-\infty}^{+\infty}\frac{U_0(x)U_0(x)}{\mathrm{par}(x)}\,\mathrm{d}x, \tag{23}$$

$$\frac{U\Psi_m}{\mathrm{par}} = \int_{-\infty}^{+\infty}\frac{U_0(x)\Psi_m(x,\rho)}{\mathrm{par}(x)}\,\mathrm{d}x, \qquad m = 1,2, \tag{24}$$

$$\frac{U\varphi_l}{\mathrm{par}} = \int_{-\infty}^{+\infty}\frac{U_0(x)\varphi_l(x,s)}{\mathrm{par}(x)}\,\mathrm{d}x, \qquad l = 1,2, \tag{25}$$

whose analytical expressions could be easily found by straightforward algebra. Note that in the computation of the first-order solution of the transverse electric field distribution, only one-dimensional integrals have to be calculated, while in the computation of the higher-order solutions two- and three-dimensional integrals are encountered.

Since the successive-order solutions of the transverse electric field distribution $\mathcal{E}(x)$ on the plane $z = 0$ have been computed, it is possible to calculate the electric field inside the waveguide as well as in the semi-infinite region $z > 0$ in terms of $\mathcal{E}(x)$. For this purpose the successive-order solutions of the expansion coefficients R_0, $R_m(\rho)$, $T_1(s)$, and $T_2(s)$ are obtained by replacing the respective solutions of $\mathcal{E}(x)$ in the following equations:

$$R_0 = -1 + \int_{-\infty}^{+\infty}\mathcal{E}(x)U_0(x)\mathrm{d}x, \tag{26a}$$

$$R_m(\rho) = \int_{-\infty}^{+\infty}\mathcal{E}(x)\Psi_m(x,\rho)\mathrm{d}x, \qquad m = 1,2, \tag{26b}$$

$$T_l(s) = \int_{-\infty}^{+\infty}\mathcal{E}(x)\varphi_l(x,s)\mathrm{d}x, \qquad l = 1,2. \tag{26c}$$

Equations (26) are derived from the boundary condition of the transverse electric field distribution on $z = 0$. Then the zero- and first-order solutions of the guided-mode reflection coefficient are given by

$$R_{00} = -1 + 2Y_1\left(\frac{UU}{\mathrm{par}}\right), \tag{27a}$$

$$R_{01} = R_{00} - 2Y_1\left\{(Y_1 - Y_{10})\left(\frac{UU}{\mathrm{par}}\right)^2 + \sum_{m=1}^{2}\int_{\rho_m}^{+\infty}[Y(\rho) - Y_{10}]\left(\frac{U\Psi_m}{\mathrm{par}}\right)^2\mathrm{d}\rho + \sum_{l=1}^{2}\int_{0}^{+\infty}[Y_0(s) - Y_{00}]\left(\frac{U\varphi_l}{\mathrm{par}}\right)^2\mathrm{d}s\right\}, \tag{27b}$$

while the second-order (R_{02}) and third-order (R_{03}) solutions of the guided-mode reflection coefficient as well as

the successive-order solutions for the other coefficients, $R_m(\rho)$ and $T_l(s)$, are omitted. Note that the zero-order solution given in Eq. (27a) corresponds to the reflection coefficient of a plane wave on the interface between two semi-infinite regions with refractive indices n_1 and n_0, respectively.

Finally, since the power of the reflected guided mode is equal to $|R_0|^2$, the respective power of the reflected radiation modes is given by

$$P_{\mathrm{rad}} = \sum_{m=1}^{2} \int_{\rho_m}^{+\infty} |R_m(\rho)|^2 \, \mathrm{d}\rho, \tag{28}$$

while the far-field radiation pattern is found to be[20]

$$\Phi_{\mathrm{II}}(r, \theta) = \sqrt{\frac{2}{k_0 n_0 r}} \exp(-jk_0 n_0 r + j\pi/4)(k_0 n_0 \cos\theta) \times \sum_{l=1}^{2} T_l(s = k_0 n_0 \sin\theta) \qquad (r \to +\infty), \tag{29}$$

where r and θ are the cylindrical coordinates ($z = r\cos\theta$ and $x = r\sin\theta$) and $0 < \theta < \pi/2$ in order that Eq. (29) defines the pattern only for $z > 0$.

3. SOLUTION BY THE VARIATIONAL TECHNIQUE

In this section the above and other problems will be solved by the approximate variational technique, which is a modification of the well-known method proposed by Schwinger for solving different problems of the metal waveguide theory.[8,13,14,22] Below we shall consider a general case, assuming that the refractive index $n(x)$ is an arbitrary function of the transverse coordinate x inside the slab ($|x| < D/2$). We shall derive the basic equations in the vector form, which is more convenient for such problems. As stated in Section 2, we shall treat a single-mode problem. Many derivations are similar to those used in the previous section; therefore we omit some details.

In the left ($z < 0$) and right ($z > 0$) regions, the fields can be written in terms of the eigenmode expansions.[13,15,23] Let us assume that $\mathbf{E}_0(1)$, $\mathbf{H}_0(1)$, $\mathbf{E}_{m\rho}(1)$, $\mathbf{H}_{m\rho}(1)$, and $\mathbf{E}_{ms}(2)$, $\mathbf{H}_{ms}(2)$ are the electric and magnetic fields of the guided mode and the radiation eigenmodes of the waveguide ($z < 0$) and the right semi-infinite region ($z > 0$), respectively, where ρ, s are the transverse wave numbers and m is the discrete index labeling the modes (for example, the even and odd modes of the right semi-infinite region). The numbers 1 and 2 in the parentheses denote the quantities related to the left and right regions. For $z < 0$ the eigenmode expansion mentioned above is

$$\mathbf{E} = [\exp(-j\beta_0 z) + R_0 \exp(+j\beta_0 z)]\mathbf{E}_0(1) + \sum_{m=1}^{2} \int_{\rho_m}^{\infty} R_m(\rho)\mathbf{E}_{m\rho}(1)\exp[j\beta(\rho)z]\,\mathrm{d}\rho, \tag{30}$$

and for $z > 0$ it is

$$\mathbf{E} = \sum_{m=1}^{2} \int_{0}^{\infty} T_m(s)\mathbf{E}_{ms}(2)\exp[-j\gamma(s)z]\,\mathrm{d}s, \tag{31}$$

where $R_m(\rho)$, $T_m(s)$ are unknown expansion coefficients and $\beta(\rho)$, $\gamma(s)$ are the propagation coefficients.

For the three-layer slab guide with a constant profile $n(x)$, the analytical representation of modes are the same as those used in Section 2. In a general case we can construct the system of the radiation modes by using the S-operator theory.[24,25] The electric field of the guided mode is given by $\mathbf{E}_0(1) = (U_0(x), 0, \mathrm{d}U_0(x)/\mathrm{d}x)/n^2(x)$, where $U_0(x)$ is the solution of the following differential equation:

$$n^2(x)\frac{\mathrm{d}}{\mathrm{d}x}\left[\frac{1}{n^2(x)}\frac{\mathrm{d}U_0}{\mathrm{d}x}\right] + [k_0{}^2 n^2(x) - \beta_0{}^2]U_0 = 0, \tag{32}$$

where β_0 is the propagation constant of the mode [see Eqs. (1)–(3)] and the function $U_0(x)$ must approach zero for $x \to \pm\infty$.

The fields of all the eigenmodes satisfy the orthogonality conditions:

$$\begin{aligned} \langle \mathbf{E}_0(1), \mathbf{H}_{m\rho}(1)\rangle &= 0, \\ \langle \mathbf{E}_{m\rho}(1), \mathbf{H}_{m'\rho'}(1)\rangle &= \delta_{mm'}\delta(\rho - \rho'), \\ \langle \mathbf{E}_0(1), \mathbf{H}_0(1)\rangle &= 1, \\ \langle \mathbf{E}_{ms}(2), \mathbf{H}_{m's'}(2)\rangle &= \delta_{mm'}\delta(s - s'), \end{aligned} \tag{33}$$

where

$$\langle \mathbf{E}, \mathbf{H}\rangle = \int_{z=0} (\mathbf{E} \times \mathbf{H}) \cdot \mathbf{e}_z \, \mathrm{d}x\mathrm{d}y. \tag{34}$$

Equations (33) can be derived from the general orthogonality relations presented in Refs. 24 and 25. Here $\mathbf{e}_z$ is the unit vector oriented along the guide axis Oz, and the skew cross indicates the vector product. Note that the unknown expansion coefficients $R_m(\rho)$, $T_m(s)$ can be expressed in terms of the facet electric (or magnetic) field with the help of the orthogonality relations presented above. Matching the transverse field components at the terminal plane $z = 0$ and utilizing the eigenmode orthogonality relations lead to the integral equation for the transverse electric field $\mathbf{E}$ [see Eqs. (15)–(17)]:

$$\hat{\Xi}_e[\mathbf{E}] = 2\mathbf{H}_{0\perp}(1), \tag{35}$$

where the integral operator $\hat{\Xi}_e$ is equal to

$$\hat{\Xi}_e[\mathbf{E}] = \langle \mathbf{E}, \mathbf{H}_{0\perp}(1)\rangle \mathbf{H}_{0\perp}(1) + \sum_{m=1}^{2} \int \langle \mathbf{E}, \mathbf{H}_{m\rho\perp}(1)\rangle \mathbf{H}_{m\rho\perp}(1)\,\mathrm{d}\rho + \sum_{m=1}^{2} \int \langle \mathbf{E}, \mathbf{H}_{ms\perp}(2)\rangle \mathbf{H}_{ms\perp}(2)\,\mathrm{d}s \tag{36}$$

and the $\perp$ sign denotes the transverse parts of the vectors. In this equation the integration limits, which depend on the waveguide structure and can be determined by the approach described in Ref. 24, have not been written.

Using a standard technique,[13,15,22] we can derive the stationary functionals for basic characteristics of the

problem in question. For instance, taking into account the expression for the reflection coefficient,

$$R_0 = -1 + \langle \mathbf{E}, \mathbf{H}_0(1) \rangle, \tag{37}$$

we obtain the following functional:

$$\frac{1 - R_0}{1 + R_0} = \frac{\langle \mathbf{E}, \hat{\Xi}_{er}[\mathbf{E}] \rangle}{\langle \mathbf{E}, \mathbf{H}_0(1) \rangle^2}, \tag{38}$$

where the new integral operator is

$$\hat{\Xi}_{er}[\mathbf{E}] = \hat{\Xi}_e[\mathbf{E}] - \langle \mathbf{E}, \mathbf{H}_{0\perp}(1) \rangle \mathbf{H}_{0\perp}(1). \tag{39}$$

Because of the stationary property of Eq. (38), sufficiently precise results can be obtained for the reflection coefficient R_0 by substituting the approximate field distribution $\mathbf{E}$. The field that is proportional to the incident one $\mathbf{E} = A\mathbf{E}_0(1)$, with A being a constant, will be used below. Note that this constant is canceled out in the following equations. Utilizing Eq. (38) for the three-layer slab waveguide leads to the expression

$$\frac{1 - R_0}{1 + R_0} = \frac{\beta_0 {n_0}^2}{\pi {Q_0}^2(1)} \int_0^{+\infty} [{Q_c}^2(s) + {Q_s}^2(s)] \times \frac{ds}{({k_0}^2 {n_0}^2 - s^2)^{1/2}}, \tag{40}$$

where

$$Q_c(s) = \int_{-\infty}^{+\infty} U_0(x) \frac{\cos(sx)}{n^2(x)} dx,$$

$$Q_s(s) = \int_{-\infty}^{+\infty} U_0(x) \frac{\sin(sx)}{n^2(x)} dx, \tag{41}$$

$${Q_0}^2(1) = \int_{-\infty}^{+\infty} \frac{{U_0}^2(x)}{n^2(x)} dx, \tag{42}$$

and $U_0(x)$ is the solution of Eq. (32). It should be noted that the functions $\mathbf{E}_0(1)$ and $\mathbf{H}_{m\rho}(1)$ are orthogonal [see Eqs. (33)]; therefore the waveguide radiation mode fields are excluded from the final results. This property of the variational solution permits the study of complicated structures, since the free-space eigenmode fields $\mathbf{E}_{ms}(2)$, $\mathbf{H}_{ms}(2)$ can be easily constructed [see Eq. (11)]. Note also that for the constant profile of the $n(x)$ the integrals Q_c and Q_s can be calculated analytically.

Based on Eq. (40) derived above, simple estimations of the reflection coefficient R_0 can be obtained for several limiting cases. For example, near cutoff, where $k_0 D \to 0$ and $h_1 \ll h_2$, $h_1 \ll h_3$, all the integrals of Eqs. (41) can be calculated analytically. As a result, the following equation is valid:

$$R_0 = (n_1 - n_0)/(n_1 + n_0). \tag{43}$$

Fresnel law can also derive the last equation if the field of the guided mode is considered near cutoff.

Equation (38) is the so-called electrical formulation of the variational principle.[13,15,22,26] With the help of the same technique, the integral equation for the magnetic field $\mathbf{H}$ at the facet plane $z = 0$ can be derived:

$$\hat{\Xi}_m[\mathbf{H}] = 2\mathbf{E}_{0\perp}(1), \tag{44}$$

Table 1. Convergence of the Reflection Coefficient for an Abruptly Ended Waveguide[a]

Method	Reflectivity $\lvert R_0 \rvert^2$
Integral equation method (zero order)	0.2499
Integral equation method (first order)	0.2741
Integral equation method (second order)	0.2701
Integral equation method (third order)	0.2697
Variational technique [Eq. (40)]	0.2687
Variational technique [Eq. (45)]	0.2181
Vassallo method (Ref. 10)	0.2638
Buus formula (Ref. 30)	0.2322

[a] For the parameters $\lambda_0 = 0.86\,\mu$m, $n_2 = 3.6$, $D = 0.2\,\mu$m, $\Delta_{12} = \Delta_{32} = 10\%$ (i.e., $n_1 = n_3 = 3.24$), and $n_0 = 1$.

where the integral operator $\hat{\Xi}_m$ is expressed in terms of the electric fields of all eigenmodes. From this equation the magnetic formulation of the variational principle for the reflection coefficient R_0 can be obtained.[15] For the problem in question, the final equation has the form

$$\frac{1 + R_0}{1 - R_0} = \frac{1}{\pi \beta_0 {n_0}^2 {Q_0}^2(1)} \times \int_0^{+\infty} [\tilde{Q}_c^2(s) + \tilde{Q}_s^2(s)] \sqrt{{k_0}^2 {n_0}^2 - s^2}\, ds, \tag{45}$$

where

$$\tilde{Q}_c(s) = \int_{-\infty}^{+\infty} U_0(x) \cos(sx) dx,$$

$$\tilde{Q}_s(s) = \int_{-\infty}^{+\infty} U_0(x) \sin(sx) dx. \tag{46}$$

Near cutoff ($k_0 D \to 0$) Eqs. (40) and (45) give similar results. However, they are not identical. Test and estimations have shown that the electrical formulation [see Eq. (40)] is more precise. Table 1 illustrates this conclusion, where the values of the square magnitude of the guided-mode reflection coefficient calculated by different methods are presented. The parameters of the problem are $\lambda_0 = 0.86\,\mu$m, $n_2 = 3.6$, $D = 0.2\,\mu$m, $\Delta_{12} = \Delta_{32} = 10\%$ (i.e., $n_1 = n_3 = 3.24$), and $n_0 = 1$. The same results are valid for other parameters.

The numerical results, presented in Section 4, are obtained with the help of the electric field formulation of the variational principle. The boundary-value problem for the guided mode on the interval $(-D/2, D/2)$ is solved by the target method.[27] Both the field distribution $U_0(x)$ and the Fourier integrals Q_c, Q_s are calculated at the same time by the adaptive Runge–Kutta procedure (with a variable step of the integrations). Finally, the reflection coefficient is computed by the general equation (40).

4. NUMERICAL RESULTS

We have performed several numerical computations by applying the theory developed in Sections 2 and 3. It should be noted that in the numerical computation of the

integrals a multisegment Gaussian quadrature procedure has been employed. Increasing the number of segments attains convergence in the numerical integrations. Finally, the following definitions are made: $\Delta_{12} = 1 - n_1/n_2$, $\Delta_{13} = 1 - n_3/n_1$, and $\Delta_{32} = 1 - n_3/n_2$.

At first we consider the problem of an abruptly terminated symmetrical slab waveguide, and we compare our results with those obtained by methods appearing in previously published works.[9–12,28–33] The results of the comparison are presented in Fig. 2, where the reflectivity $|R_0|^2$ of the dominant TM guided mode is plotted as a function of the core width D (slab thickness) for a waveguide geometry with $\lambda_0 = 0.86\,\mu$m, $n_2 = 3.6$, and $n_0 = 1$. In Fig. 2(a) we have chosen $n_1 = n_3 = 3.492$ (i.e., $\Delta_{12} = \Delta_{32} = 3\%$, $\Delta_{13} = 0\%$), and in Fig. 2(b), we have chosen $n_1 = n_3 = 3.24$ (i.e., $\Delta_{12} = \Delta_{32} = 10\%$, $\Delta_{13} = 0\%$). From these figures it is clear that results obtained by using the first- and second-order solutions of the integral equation method are in very good agreement with those of the variational method. It should also be mentioned that most of the methods derived in the publications given in Fig. 2 are approximate. Furthermore,

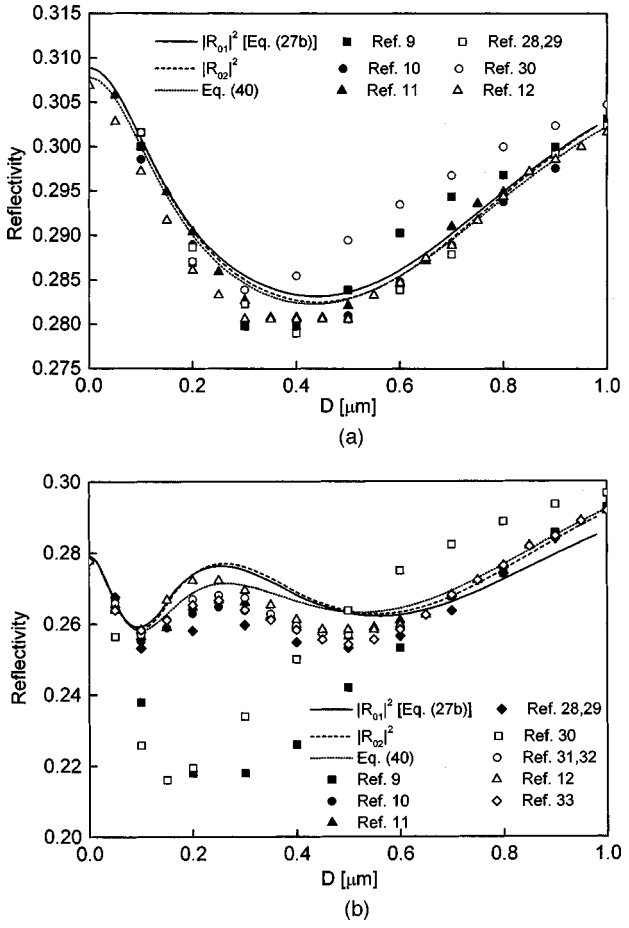

Fig. 2. (a) Comparison of the results obtained by using the two methods presented in this paper with others appearing in previously published works for an abruptly terminated symmetrical slab waveguide with $\lambda_0 = 0.86\,\mu$m, $n_2 = 3.6$, $n_0 = 1$, and $n_1 = n_3 = 3.492$ ($\Delta_{12} = \Delta_{32} = 3\%$, $\Delta_{13} = 0\%$). (b) Similar to (a) but applies to the problem with the parameters $\lambda_0 = 0.86\,\mu$m, $n_2 = 3.6$, $n_0 = 1$, and $n_1 = n_3 = 3.24$ ($\Delta_{12} = \Delta_{32} = 10\%$, $\Delta_{13} = 0\%$).

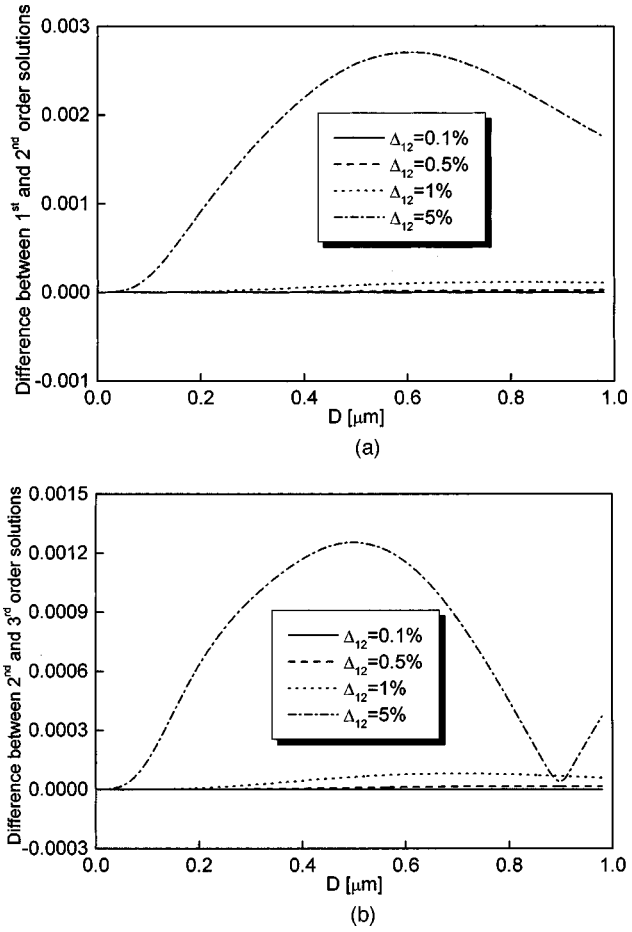

Fig. 3. (a) Difference between the first- and second-order solutions of the integral equation method for an abruptly terminated symmetrical slab waveguide with $\lambda_0 = 0.9\,\mu$m, $n_2 = 3.6$, $n_0 = 1$, and $\Delta_{12} = \Delta_{32} = 0.1\%$, 0.5%, 1%, and 5%. (b) Similar to (a) but for the difference between the second- and third-order solutions.

the data presented in these figures are close for all values of the core width D, except the range $0.1 < D < 0.3$. Nevertheless, the difference between all the results observed in that width range decreases if the value $\Delta_{12} \to 0$.

Next, a comparison of the successive-order solutions of the integral equation method is performed in order to study its convergence. In Fig. 3 we present the difference between the successive-order solutions as a function of the core width D, with the relative refractive-index difference Δ_{12} as a parameter, for an abruptly terminated symmetrical slab waveguide with $\lambda_0 = 0.9\,\mu$m, $n_2 = 3.61$, $n_0 = 1$, and $\Delta_{12} = \Delta_{32} = 0.1\%$, 0.5%, 1%, and 5%. From these figures it is obvious that the difference becomes smaller as Δ_{12} decreases, especially near cutoff.

We now consider asymmetrical structures. In all the numerical computations considered below, the following values have been chosen: $\lambda_0 = 0.9\,\mu$m, $n_2 = 3.61$, and $n_0 = 1$. In Fig. 4 the very good agreement between the two methods employed in this paper is exhibited. In particular, we present the variation of the reflectivity $|R_0|^2$ of the dominant TM guided mode with the core width D for two cases, one with $\Delta_{12} = 1\%$, $\Delta_{32} = 10\%$ [Fig. 4(a)] and the other with $\Delta_{12} = 5\%$, $\Delta_{32} = 10\%$ [Fig. 4(b)]. From

these figures it is clear that the results obtained by the variational technique (squares) coincide with the higher-order solutions of the integral equation method (solid, long-dashed, and dotted curves), especially when the weak guidance condition is satisfied [see Fig. 4(a)]. Furthermore, the two horizontal short-dotted and dotted–dashed lines correspond to the cases of the reflection between two semi-infinite spaces with refractive indices n_1, n_0 and n_2, n_0, respectively. The lower of them corresponds to the near-cutoff regime obtained by Eq. (43), and the higher one corresponds to the asymptotic value $k_0D \rightarrow +\infty$. Finally, we give the results obtained by using the effective refractive-index formula (EFIF), i.e., by using the equation $R_0 = (\beta_0 - k_0n_0)/(\beta_0 + k_0n_0)$ (short-dashed curve).

In Fig. 5(a) we present the variation of the magnitudes of the transverse electric field distribution $|\mathcal{E}(x)|$ (solid curve) and the guided-mode transverse electric field distribution, i.e., $|(1 + R_0)U_0(x)|/n^2(x)$ (dashed curve), with the normalized transverse distance x/D on the terminal plane $z = 0$ for a slab waveguide with $D = 0.5\,\mu$m and

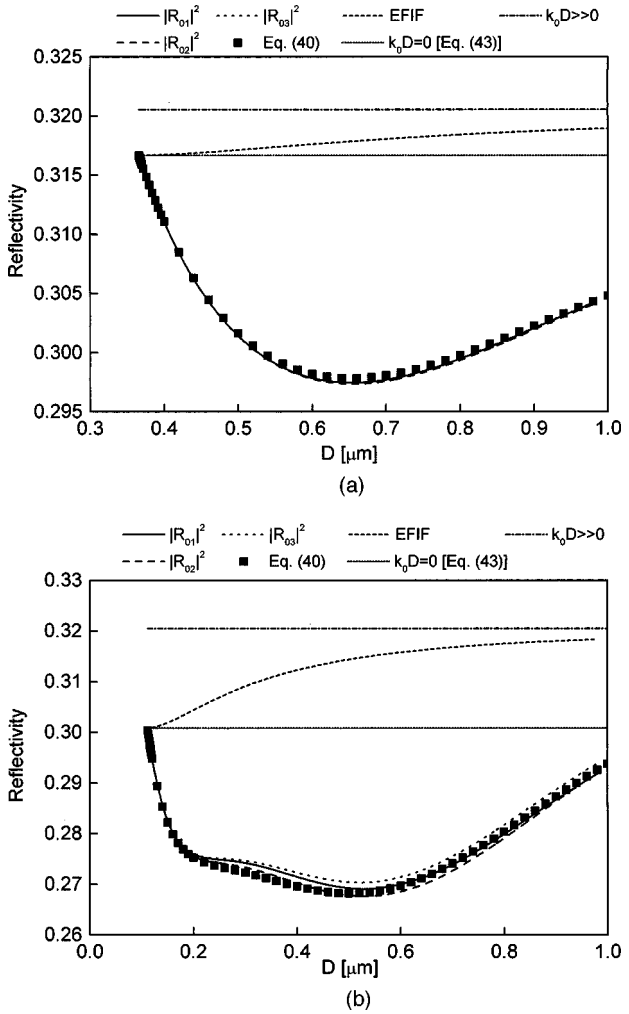

Fig. 4. (a) Variation of the reflectivity $|R_0|^2$ of the dominant TM guided mode with the core width D for an abruptly terminated asymmetrical slab waveguide with $\lambda_0 = 0.9\,\mu$m, $n_2 = 3.61$, $n_0 = 1$, $\Delta_{12} = 1\%$, and $\Delta_{32} = 10\%$. (b) Similar to (a) but applies to the problem with the parameters $\lambda_0 = 0.9\,\mu$m, $n_2 = 3.61$, $n_0 = 1$, $\Delta_{12} = 5\%$, and $\Delta_{32} = 10\%$.

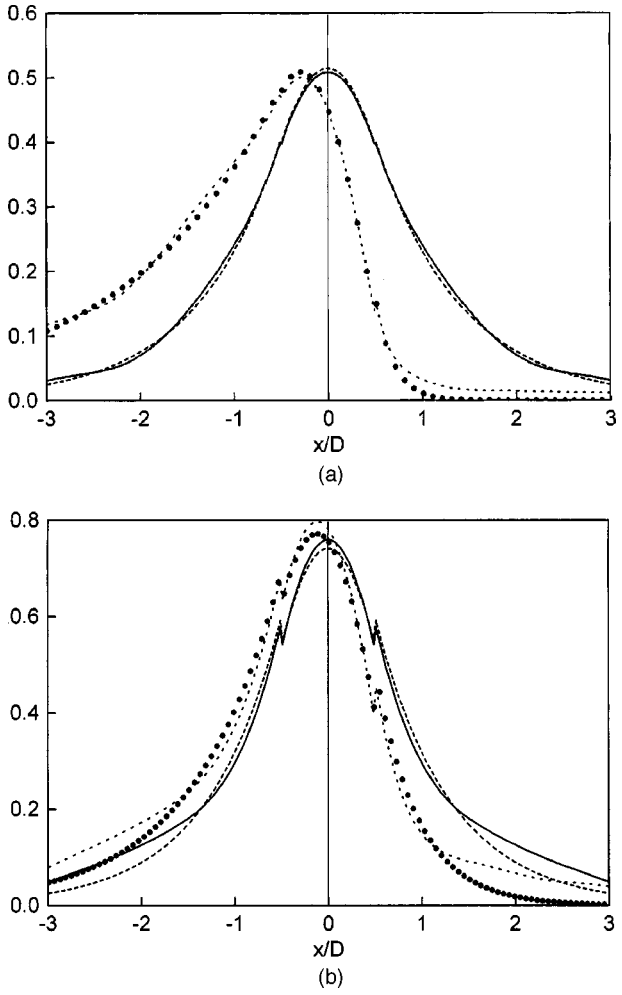

Fig. 5. (a) Variation of the magnitude of the transverse electric field distribution $|\mathcal{E}(x)|$ (solid curve) and the transverse electric field distribution of the guided mode, $|(1 + R_0)\ U_0(x)|/n^2(x)$ (dashed curve), at the plane $z = 0$ with the normalized transverse distance x/D for a slab waveguide with $\lambda_0 = 0.9\ \mu$m, $n_2 = 3.61$, $D = 0.5\ \mu$m, $n_0 = 1$, and $\Delta_{12} = \Delta_{32} = 1\%$. Also given is the variation of $|\mathcal{E}(x)|$ (dotted curve) and $|(1 + R_0)U_0(x)|/n^2(x)$ (circles) for the same geometry but with $\Delta_{12} = 1\%$, $\Delta_{32} = 10\%$. (b) Variation of the magnitude of the transverse electric field distribution $|\mathcal{E}(x)|$ (solid curve) and the transverse electric field distribution of the guided mode, $|(1 + R_0)U_0(x)|/n^2(x)$ (dashed curve), at the plane $z = 0$ with the normalized transverse distance x/D for a slab waveguide with $\lambda_0 = 0.9\ \mu$m, $n_2 = 3.61$, $D = 0.25\ \mu$m, $n_0 = 1$, and $\Delta_{12} = \Delta_{32} = 5\%$. Also given is the variation of $|\mathcal{E}(x)|$ (dotted curve) and $|(1 + R_0)U_0(x)|/n^2(x)$ (circles) for the same geometry but with $\Delta_{12} = 5\%$, $\Delta_{32} = 10\%$.

$\Delta_{12} = \Delta_{32} = 1\%$. Obviously, in that case the waveguide is symmetrical; therefore the curves $|\mathcal{E}(x)|$ and $|(1 + R_0)U_0(x)|/n^2(x)$ are also symmetrical with respect to the plane $x = 0$, as is expected. Since these two curves are almost identical, the contribution of the radiation modes to the transverse electric field distribution on the plane $z = 0$ is negligible. It should be mentioned that the transverse electric field distribution is not continuous at the core–clad interface ($x = \pm D/2$), as is expected from the boundary conditions. In the same figure the corresponding curves of an asymmetrical slab waveguide are also drawn for a waveguide with the same param-

eters, except that $\Delta_{12} = 1\%$ and $\Delta_{32} = 10\%$. From the last two curves, the asymmetrical behavior of $|\mathcal{E}(x)|$ (dotted curve) and $|(1 + R_0)U_0(x)|/n^2(x)$ (circles) is exhibited. The same variations are presented in Fig. 5(b) for a waveguide with $D = 0.25\,\mu$m and $\Delta_{12} = \Delta_{32} = 5\%$ (solid and dashed curves) and $\Delta_{12} = 5\%$, $\Delta_{32} = 10\%$ (dotted curve and circles). Obviously, in this case the asymmetrical behavior of the electric field is smaller than in the previous case, because of the larger value of Δ_{12}, with the result that most of the field distribution and the guided power is in the core region $|x| < D/2$. Furthermore, in the last case the discontinuity of $|\mathcal{E}(x)|$ and $|(1 + R_0)U_0(x)|/n^2(x)$ at the core–clad interface is larger than in the previous case because of the larger value of Δ_{12}.

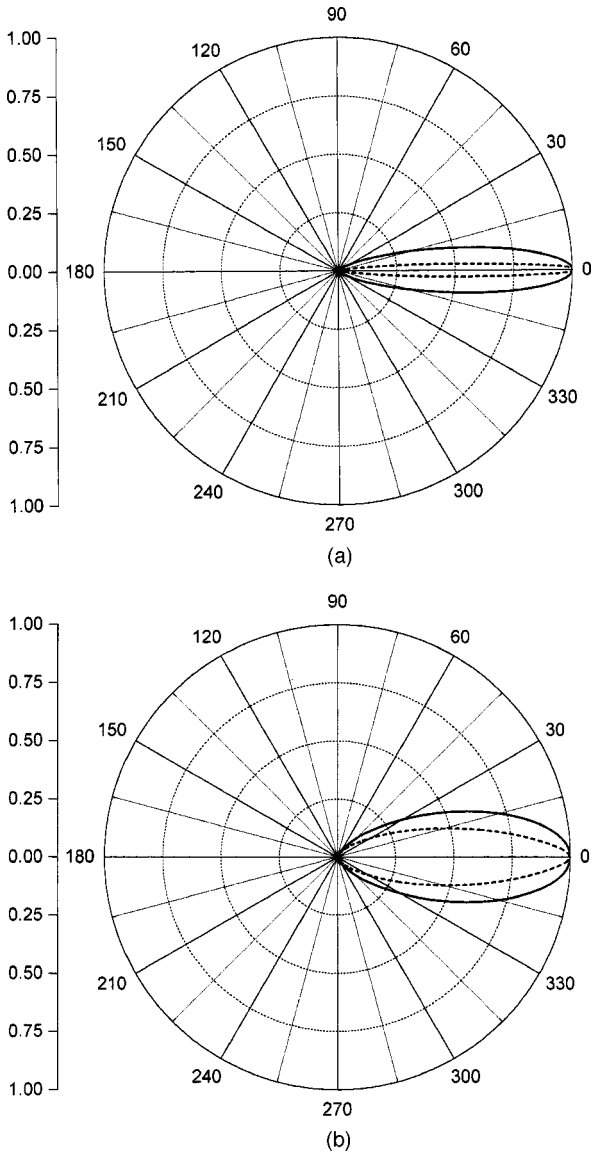

Fig. 6. (a) Normalized radiation pattern for an abruptly terminated slab waveguide with $\lambda_0 = 0.9\ \mu$m, $n_2 = 3.61$, $D = 0.5\ \mu$m, $n_0 = 1$, and $\Delta_{12} = \Delta_{32} = 1\%$ (solid curve) and $\Delta_{12} = 1\%$, $\Delta_{32} = 10\%$ (dashed curve). (b) Similar to (a) but applies to the problem with the parameters $\lambda_0 = 0.9\ \mu$m, $n_2 = 3.61$, $D = 0.25\ \mu$m, $n_0 = 1$, and $\Delta_{12} = \Delta_{32} = 5\%$ (solid curve) and $\Delta_{12} = 5\%$, $\Delta_{32} = 10\%$ (dashed curve).

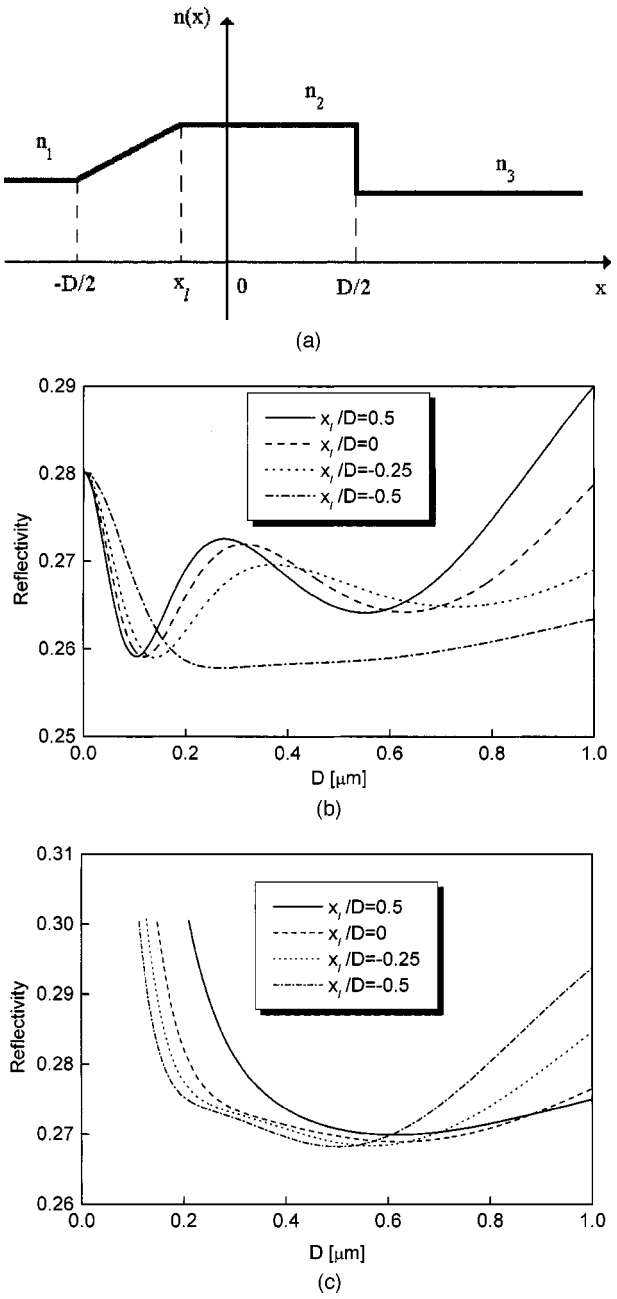

Fig. 7. (a) Variation of the refractive index $n(x)$, which is assumed to change linearly from n_1 to n_2 on the interval $(-D/2,\ x_l)$. (b) Variation of the reflectivity $|R_0|^2$ of the dominant TM guided mode with the core width D for an abruptly terminated symmetrical slab with $\lambda_0 = 0.9\ \mu$m, $n_2 = 3.61$, $\Delta_{12} = \Delta_{32} = 10\%$, and $n_0 = 1$ and with linearly varying refractive index from n_1 to n_2 on the interval $(-D/2, x_l)$ as shown in (a). (c) Variation of the reflectivity $|R_0|^2$ of the dominant TM guided mode with the core width D for an abruptly terminated asymmetrical slab with $\lambda_0 = 0.9\,\mu$m, $n_2 = 3.61$, $\Delta_{12} = 5\%$, $\Delta_{32} = 10\%$, and $n_0 = 1$ and with linearly varying refractive index from n_1 to n_2 on the interval $(-D/2, x_l)$ as shown in (a).

As a consequence, the far-field radiation patterns for these cases are different [Figs. 6(a) and 6(b)]. Specifically, the radiation pattern of the first waveguide [Fig. 6(a)] is narrower (i.e., smaller value of the 3-dB angle and therefore larger directivity) than that of the second [Fig. 6(b)]. In addition, for the system under consideration the

far-field pattern is asymmetrical rather than symmetrical. However, under weak guidance conditions this asymmetry is very small. For example, for the parameters used in Fig. 6 the value of the angle $\theta_{\max}$, which corresponds to the maximum value of the far-field pattern, is approximately 0.1°–0.5° (different from $\theta_{\max} = 0°$ of the symmetrical waveguide).

To demonstrate the potential of the variational technique, we examine the effect of the transition (diffusion) layer of the waveguide refractive-index profile on the reflectivity features. The refractive index $n(x)$ is assumed to change linearly from n_1 to n_2 on the interval $(-D/2, x_l)$, as shown in Fig. 7(a). Figures 7(b) and 7(c) present the reflectivity $|R_0|^2$ for such structures. The drawn curves correspond to the cases $x_l = 0.5D$ (solid curve), $x_l = 0$ (dashed curve), $x_l = -0.25D$ (dotted curve), and $x_l = -0.5D$ (dotted–dashed curve, i.e., for the step profile). The problem parameters are $\lambda_0 = 0.9\,\mu$m, $n_2 = 3.61$, $n_0 = 1$, and $\Delta_{12} = \Delta_{32} = 10\%$ [Fig. 7(b)] and $\Delta_{12} = 5\%$, $\Delta_{32} = 10\%$ [Fig. 7(c)]. From these figures it is obvious that asymmetry of the refractive-index values n_1 and n_3 is seen to change the reflective characteristics.

5. DISCUSSION

The results for the TM problem, presented above, sufficiently differ from those for the similar TE problem.[20] Near cutoff the reflection coefficient $|R_0|$ of the TM mode is smaller than its initial value [see Eq. (43)], whereas for the TE mode it is larger than this value. For the symmetrical geometry this effect can be explained by using the Fresnel law.[30] This explanation is also suitable for the asymmetrical problem. However, in the asymmetrical case the reflectivity dependencies on the problem parameters are more complicated, since these parameters can also shift the mode cutoff frequencies.

In the TM and TE problems, the field structures at the terminal planes are also different. For the first problem the scattering of the waves by the edge points ($x = \pm D/2, z = 0$) plays a more important role than for the second problem. Below, we briefly consider this item by using the results of Meixner's theory[34] and its modification.[26] For simplicity, we shall treat the symmetrical case ($n_1 = n_3$). Estimations, based on the above papers, show that the electric field at the terminal plane $z = 0$ has the following approximate representation:

$$E_x(x, 0) = F_1(x) + F_2(x)\Delta_{12} r_e^{-a}/\ln(k r_e), \qquad (47)$$

where

$$r_e = \sqrt{|x^2 - D^2/4|}, \qquad a \approx \sqrt{2\Delta_{12}}/[\pi(n_0^2 + n_2^2)]. \qquad (48)$$

Here F_1 and F_2 are piecewise regular functions, which are liable to steps in the points $x = \pm D/2$. For the TM problem the electric field is seen to be singular in the edge points. Under the weak guidance condition the power constant a is very small; for example, assuming that $n_2 = 3.61$, $\Delta_{12} = 10\%$, and $n_0 = 1$, we have $a \approx 0.01$. In this case the singularities are small; nevertheless, they complicate the solution of the problem.

Using the above formulas, we can make our conclusions, dealing with the convergence of the technique described in Section 2, more accurate. Since the electric field on the terminal plane is irregular, all the integrals of the eigenmode expansions [see Eqs. (8) and (10)] converge only in the mean. From Eq. (47) it follows that the expansion coefficients $R_m(\rho)$ and $T_l(s)$ contain small terms, which slowly approach zero when $\rho \to +\infty$ and $s \to +\infty$. The existence of these terms slows the convergence of the iteration procedure, especially in the vicinity of the points $x = \pm D/2$ (see Fig. 5). However, if $\Delta_{12} \ll 1$, the second singular term in Eq. (47) is small and its influence is negligible. Since the singular regions (near the edge points) are very narrow, they make small contributions to all the integral characteristics of the problem, such as the reflection coefficient, etc. It seems that the convergence of the technique can be improved if we use the terminal field described by Eq. (47) as the first-order solution. Nevertheless, this subject requires further consideration.

Note that for the TE problem, only high derivatives of the electric field at the terminal plane are singular. In this case the field is continuous; for example, for $x \to D/2$ we have

$$|E_x(x, 0) - E_x(D/2, 0)| \sim \Delta_{12} r_e^2 \ln(k r_e). \qquad (49)$$

Therefore, for this problem, the difficulties mentioned above are removed, and the conditions required for Δ_{12} are less drastic.[20]

6. CONCLUSION

The scattering phenomenon from an abruptly terminated asymmetrical slab waveguide has been studied by both the integral equation method and the variational technique. The reflection coefficient of the dominant TM guided mode, the far-field radiation pattern, and the transverse electric field distribution on the terminal plane $z = 0$ are computed. Both methods employed in this problem are based on the same integral equation, and they seem to be able to complement each other. Based on the analysis developed in Sections 2 and 3, several numerical computations have been performed, including the three-layer slab waveguide and the structure with variable profile of the core refractive index. From the numerical results it has been found that the two methods are in very good agreement, especially under the weak guidance condition, while a comparison with previously published works has been performed and presented. Furthermore, the reflectivity properties of the asymmetrical structures are found to differ from those of symmetrical ones, i.e., the phase asymmetry of the field distribution on the terminal plane. Of course, this effect is small under the weak guidance conditions, and therefore the displacement of the radiation pattern (with respect to $\theta = 0°$) is also small. Finally, it should be mentioned that in the case of TM modes, unlike that of TE modes, the transverse electric field distribution is discontinuous at the core–clad interface ($x = \pm D/2$).

ACKNOWLEDGMENTS

The authors thank C. Vassallo for the data presented in Table 1 as the Vassallo method. A. B. Manenkov also thanks P. C. Kendall for useful discussions. This work has been partly funded by the Special Account of Research of the University of Athens.

Address correspondence to I. G. Tigelis at the location on the title page or by e-mail, itigelis@cc.uoa.gr.

REFERENCES

1. D. Marcuse, "Radiation losses of tapered dielectric slab waveguides," Bell Syst. Tech. J. **49**, 273–290 (1970).
2. G. H. Brooke and M. M. Z. Kharadly, "Step discontinuities on dielectric waveguides," Electron. Lett. **12**, 473–475 (1976).
3. T. E. Rozzi, "Rigorous analysis of the step discontinuity in a planar dielectric waveguide," IEEE Trans. Microwave Theory Tech. **MTT-26**, 738–746 (1978).
4. K. Morishita, S. Inagaki, and N. Kumagai, "Analysis of discontinuities in dielectric waveguides by means of the least squares boundary residual method," IEEE Trans. Microwave Theory Tech. **MTT-27**, 310–315 (1979).
5. A. Ittipiboon and M. Hamid, "Scattering of surface waves at a slab waveguide discontinuity," Proc. Inst. Electr. Eng. **126**, 798–804 (1979).
6. H. Yajima, "Coupled mode analysis of dielectric planar branching waveguides," IEEE J. Quantum Electron. **QE-14**, 749–755 (1978).
7. K. Uchida and K. Aoki, "Scattering of surface waves on transverse discontinuities in symmetrical three-layer dielectric waveguides," IEEE Trans. Microwave Theory Tech. **MTT-32**, 11–19 (1984).
8. C. M. Angulo, "Diffraction of surface waves by a semi-infinite dielectric slab," IRE Trans. Antennas Propag. **AP-5**, 100–109 (1957).
9. T. Ikegami, "Reflectivity of mode at facet and oscillation mode in double-heterostructure injection lasers," IEEE J. Quantum Electron. **QE-8**, 470–476 (1972).
10. C. Vassallo, "Reflectivity of multi-dielectric coatings deposited on the end facet of a weakly guiding dielectric slab waveguide," J. Opt. Soc. Am. A **5**, 1918–1928 (1988).
11. P. C. Kendall, D. A. Roberts, P. N. Robson, M. J. Adams, and M. J. Robertson, "Semiconductor laser facet reflectivities using free-space radiation modes," IEE Proc. J **140**, 49–55 (1993).
12. Y. P. Chiou and H. C. Chang, "Analysis of optical waveguide discontinuities using Pade approximants," IEEE Photonics Technol. Lett. **9**, 964–966 (1997).
13. A. B. Manenkov, "Propagation of a surface wave along a dielectric waveguide with an abrupt change of parameters. II: Solution by variational method," Radiophys. Quantum Electron. **25**, 1050–1055 (1982).
14. A. B. Manenkov, "Step discontinuities in dielectric waveguides (fibres)," Opt. Quantum Electron. **22**, 65–76 (1990).
15. A. B. Manenkov, "Reflection of the surface mode from an abruptly ended W-fibre," IEE Proc. J **139**, 101–104 (1992).
16. T. J. M. Boyd, I. Moshkun, and I. M. Stephenson, "Radiation losses due to discontinuities in asymmetric three-layer optical waveguides," Opt. Quantum Electron. **12**, 143–158 (1980).
17. A. B. Manenkov, "Comparison of approximate methods of computing diffraction of waves at diameter discontinuity in a dielectric waveguide," Izv. Vyssh. Uchebn. Zaved. Radiofiz. **28**, 743–752 (1985).
18. C. N. Capsalis, N. K. Uzunoglu, and I. G. Tigelis, "Coupling between two abruptly terminated single-mode optical fibers," J. Opt. Soc. Am. B **5**, 1624–1630 (1988).
19. C. N. Capsalis and N. K. Uzunoglu, "Coupling between an abruptly terminated optical fiber and a dielectric planar waveguide," IEEE Trans. Microwave Theory Tech. **MTT-35**, 1043–1051 (1987).
20. I. G. Tigelis and A. B. Manenkov, "Scattering from an abruptly terminated asymmetrical slab waveguide," J. Opt. Soc. Am. A **16**, 523–532 (1999).
21. D. Marcuse, *Theory of Dielectric Optical Waveguide*, 2nd ed. (Academic, London, 1991), Chap. 1.
22. L. Lewin, *Theory of Waveguides* (Newness-Butterworth, London, 1975).
23. A. B. Manenkov, "Accuracy of approximations for fibre discontinuity analysis," Opt. Quantum Electron. **23**, 81–90 (1991).
24. A. B. Manenkov, "Eigenmodes expansion in lossy open waveguides (fibres)," Opt. Quantum Electron. **23**, 621–632 (1991).
25. A. B. Manenkov, "Irregular magneto-optical waveguides," IEEE Trans. Microwave Theory Tech. **MTT-29**, 906–910 (1981).
26. A. D. Vasil'ev and A. B. Manenkov, "Diffraction of the surface wave at the end of the dielectric tube," Radiophys. Quantum Electron. **30**, 320–326 (1987).
27. T. Y. Na, *Computational Methods in Engineering Boundary Value Problems* (Academic, New York, 1979).
28. F. K. Reinhart, I. Hayashi, and M. B. Panish, "Mode reflectivity and waveguide properties of double-heterostructure injection lasers," J. Appl. Phys. **42**, 4466–4479 (1971).
29. J. K. Butler and J. Zoroofchi, "Radiation fields of GaAs-(AlGa)As injection lasers," IEEE J. Quantum Electron. **QE-10**, 809–815 (1974).
30. J. Buus, "Analytic approximation for the reflectivity of DH lasers," IEEE J. Quantum Electron. **QE-17**, 2256–2257 (1981).
31. C. Vassallo, "Antireflection coatings for optical semiconductor amplifiers: justification of a heuristic analysis," Electron. Lett. **24**, 61–62 (1988).
32. A. G. Failla, G. P. Bava, and I. Montrosset, "Structural design criteria for polarization insensitive semiconductor optical amplifiers," J. Lightwave Technol. **8**, 302–308 (1990).
33. Q. Liu and W. C. Chew, "Analysis of discontinuities in planar dielectric waveguides: an eigenmode propagation method," IEEE Trans. Microwave Theory Tech. **39**, 422–429 (1991).
34. J. Meixner, "The behavior of electromagnetic fields at edges," IEEE Trans. Antennas Propag. **AP-20**, 442–446 (1972).